Atomic Force Microscopy Investigation of Fibroblasts Infected with Wild-Type and Mutant Murine Leukemia Virus (MuLV)

Yurii G. Kuznetsov, Shoibal Datta, Natantara H. Kothari, Aaron Greenwood, Hung Fan, and Alexander McPherson

Department of Molecular Biology and Biochemistry and Cancer Research Institute, University of California, Irvine, California 92697-3900 USA

ABSTRACT NIH 3T3 cells were infected in culture with the oncogenic retrovirus, mouse leukemia virus (MuLV), and studied using atomic force microscopy (AFM). Cells fixed with glutaraldehyde alone, and those postfixed with osmium tetroxide, were imaged under ethanol according to procedures that largely preserved their structures. With glutaraldehyde fixation alone, the lipid bilayer was removed and maturing virions were seen emerging from the cytoskeletal matrix. With osmium tetroxide postfixation, the lipid bilayer was maintained and virions were observable still attached to the cell surfaces. The virions on the cell surfaces were imaged at high resolution and considerable detail of the arrangement of protein assemblies on their surfaces was evident. Infected cells were also labeled with primary antibodies against the virus *env* surface protein, followed by secondary antibodies conjugated with colloidal gold particles. Other 3T3 cells in culture were infected with MuLV containing a mutation in the gPr80^{gag} gene. Those cells were observed by AFM not to produce normal MuLV on their surfaces, or at best, only at very low levels. The cell surfaces, however, became covered with tubelike structures that appear to result from a failure of the virions to properly undergo morphogenesis, and to fail in budding completely from the cell's surfaces.

INTRODUCTION

MuLV is an oncogenic retrovirus that produces leukemias in mice and rats (Gross, 1951). It is among the earliest and most thoroughly studied of the oncogenic viruses (Gross, 1970; Gardner, 1980). It can be propagated in cultured murine cells such as National Institutes of Health 3T3 fibroblasts (Weiss, 1982). The genetics, biological properties, and what is known of its structure and assembly have been reviewed elsewhere (Pincus, 1980; Stephenson, 1980; Weiss et al., 1982; Levy, 1992). Some of the properties of the virus are, however, particularly relevant to the investigation described here.

The virion of MuLV classifies it as a C-type virus, which assembles at the surface of infected cells, and acquires a plasma membrane envelope as it buds from a cell (Fine and Schochetman, 1978; Coffin, 1992). The envelopes also contain a viral encoded transmembrane protein (*env*) involved in target cell recognition and binding. At the center of the virion is a protein capsid containing two identical, single strands of genomic RNA, plus essential reverse transcriptase enzymes, as well as some accessory molecules (Lowey, 1985; Wagner and Hewlett, 1999). The protein capsid, composed of protein coded by the gene (*gag*), may or may not be of icosahedral design, but has regular geometric character (Levy, 1992; Luciw and Leung, 1992; Wagner and Hewlett, 1999). Between the lipid envelope, with its embedded protein molecules, and the protein capsid are matrix proteins that are less well characterized, but form a relatively dense layer between the two.

The mature, extracellular C-type particles are, from EM, roughly 80–120 nm in diameter (Lowey, 1985), and they present polymorphic, irregular images in electron micrographs (Murphy, 1985). These suggest that the precise structure of virions may vary between particles, and that they may be somewhat deformable.

One mutant of MuLV that has been isolated and described is in the gene for a normally glycosylated protein gPr80^{gag}, a protein that is not essential for infectivity, but is apparently important in the morphogenesis of virions (Evans et al., 1977; Edwards and Fan, 1979; Schultz et al., 1979; Neil et al., 1980). Biochemically, gPr80^{gag} is a Type II integral membrane protein that incorporates into the host cell membrane at sites of virus production (Fujisawa et al., 1997). The protein cannot be detected in free virus particles and is thought to be important in assembly or maturation. The mutant protein product of gPr80^{gag} cannot be glycosylated as can the wild-type protein.

The study we present here, using atomic force microscopy (AFM), is a comparison of 3T3 cells in culture, which are infected with wild-type MuLV, and cells infected with virus containing the gPr80^{gag} mutation. Here we examine with AFM the normal budding of wild-type virions from cell surfaces, and the anomalous forms observed on mutant MuLV infected cell surfaces.

Submitted June 20, 2002, and accepted for publication September 30, 2002.

Address reprint requests to Alexander McPherson, Department of Molecular Biology and Biochemistry, University of California, Irvine, CA 92697-3900. Tel.: 949-824-1931; Fax: 949-824-1954; E-mail: amcphers@uci.edu.

0006-3495/02/12/3665/10 $2.00

MATERIALS AND METHODS

Cell lines and viruses

43-D and 17-5 are National Institutes of Health 3T3 fibroblasts stably infected with wild-type M-MuLV and Ab-X-MLV (Fan et al., 1983; Hanecak et al., 1986), respectively, and were maintained in Dulbecco's modified Minimal Essential Eagle's Medium (DMEM) containing 10%

calf serum and antibiotics. PA317/BAG cells are PA317 cells (Miller and Buttimore, 1986) transfected with an M-MuLV-based vector expressing bacterial β-galactosidase (Price et al., 1987). They were maintained in DMEM containing 10% fetal bovine serum and antibiotics and 400 μg/ml G418. PA317/BAG cells were transfected by a plasmid containing the $gPr80^{gag}$ coding sequence (nt 357-2235) cloned into the mammalian expression vector pZeoSV (Invitrogen, San Diego, CA).

Atomic force microscopy

AFM instruments and procedures used in this investigation have been previously described for application to both cells (Kuznetsov et al., 1997b) and viruses (Kuznetsov et al., 2001). For imaging virus-infected cells, NIH 3T3 cells were grown on glass coverslips and were fixed for 15 min in a 0.05% solution of glutaraldehyde in PBS. In some cases the cells were postfixed for 90 min in a solution of 1% osmium tetroxide in PBS (Cann, 1999). After fixation, coverslips were washed with PBS and attached to metallic packs with double-sided tape. Coverslips with fixed cells were mounted on a J-piezoscanner of an atomic force microscope equipped with a fluid cell (Nanoscope III; Digital Instruments, Santa Barbara, CA). Before imaging, fixed cells were dehydrated by washing the fluid cell with 30, 50, 70, 95, and 100% solutions of ethanol for 15 min each. Treatment with ethanol removes the lipids from the membranes of both cells and virions, but leaves behind skeletal proteins of the membranes (Bennett, 1982; Hartwig and DeSisto, 1991) when fixation is with glutaraldehyde alone. Osmium tetroxide postfixation, however, cross-links the membrane lipids as well as the proteins, and the lipids are, therefore, not removed by alcohol exposure. This additionally preserves membrane-associated proteins as well.

For immunolabeling of MuLV-infected cells, the cells in PBS were first fixed with 1% paraformaldehyde for 30 min. Paraformaldehyde, unlike glutaraldehyde, preserves the immunogenicity of the cell surface proteins and virus proteins. It is commonly used in other applications of immunolabeling. The cells were washed three times with PBS and exposed to 2% normal goat serum in PBS for 30 min. The cells were then exposed for 30 min to the *env* protein antibody, made in rabbits and carried in 2% goat serum diluted with PBS, and then washed with 0.1% goat serum in PBS.

The secondary goat-anti-rabbit antibody (Ted Pella, Inc., Redding CA), diluted 1:10 in 0.1% goat serum in PBS, was added to the cells and allowed to incubate for 60 min, followed by washing in 0.1% goat serum in PBS. The cells were then postfixed with 1% OsO_4 in H_2O and washed three times in H_2O. Dehydration was then carried out as above in sequential baths of 30%, 50%, 70%, 95%, and finally 100% ethanol. Fifteen-minute exposures were utilized at each step.

Cantilevers with oxide-sharpened silicon nitride tips were 100 μm long. Images were collected in tapping, height mode at frequencies of $\sim$9.2 kHz with a scanning frequency of 1 Hz. Imaging of isolated virus was carried out by depositing a drop of sucrose gradient purified virus on freshly cleaved mica and air-drying, or alternatively, fixing with glutaraldehyde as above before air-drying. Scanning was performed under ethanol using the conditions described above.

In evaluating atomic force micrographs certain things should be borne in mind (Kuznetsov et al., 1997a). The height resolution of the instrument is extremely good, accurate to within a few angstroms even for soft biological specimens. The lateral resolution is much less precise because of the finite width of the scanning tip, generally no better than $\sim$10%. Furthermore, again because of the finite tip dimensions, isolated objects protruding above the background in AFM images appear broader than their true dimensions. For this reason, the dimensions of spherical and cylindrical objects are quantitated according to their heights above the background surface (Kuznetsov et al., 2001).

There is no evidence that the gentle fixation with glutaraldehyde used here appreciably disturbs the structures of the cell and virus surfaces, at least to the resolution of these AFM studies. For example, we and others have fixed numerous protein and virus crystals with the same low concentrations of glutaraldehyde, and these show no significant loss of resolution, increased mosaicity, or change in x-ray diffraction intensity distribution. We have also, in previous studies (Kuznetsov et al., 2001), examined plant virus crystals under ethanol (even without glutaraldehyde fixation) and see no obvious alteration in their surface structures compared to x-ray crystallography-determined structures, again to the resolution of the AFM images.

RESULTS

Living NIH 3T3 cells form a normal monolayer and, when imaged under culture media using contact mode AFM, they show the same properties as were observed in earlier AFM studies (Kuznetsov et al., 1997b). In particular, cytoskeletal fibers and filaments lying immediately below cell surfaces are clearly evident. The cells, though yielding clear and reproducible images in low magnification scans, i.e., $>\sim 10$ μ^2, proved too plastic when higher-magnification, smaller-area scans were attempted. As the tip pressure increases on smaller areas of the cell, even with tapping mode, one no longer observes surface features exclusively, but also structures lying beneath the cell surface. This is clear from the appearance of cytoskeletal elements, deformation of the surface, and irreproducibility among multiple scans of the same area. This was true in the absence of fixation even if the cells were dehydrated and imaged under ethanol. We found, however, that cells could be fixed with very low concentrations of glutaraldehyde (0.01%) or paraformaldehyde (0.01%) and then imaged in a dehydrated state under ethanol. Under these conditions, although the cells were no longer alive, their mechanical properties were sufficiently improved that they yielded clear and detailed images of the cell surfaces, which were entirely reproducible from scan to scan. An image of a cell fixed with glutaraldehyde and scanned under ethanol is shown in Fig. 1 *a*.

In Fig. 1, *b–d* are moderately high magnification images of the surfaces of a variety of 3T3 cells infected with wild-type MuLV showing the emergence of virions from cell surfaces, presumably in late stages of morphogenesis, or actually in the process of budding. Some particles may also be complete virions, which remain adsorbed to the cell surface. It is interesting to note in passing the extremely granular nature of the cell surfaces and the glutaraldehyde cross-linked networks of proteins of which they are constructed. In the images, the cell surface proteins, of various sizes and constitutions, appear as roughly spherical units, as would be expected of globular and extended proteins aggregated in linear and branched arrays. These granular assemblies are characteristic of all of the glutaraldehyde-treated cell surfaces we have investigated and are not specific to these cells alone. In other investigations using scanning tunneling electron microscopy (Bennett, 1982; Hartwig and DeSisto, 1991), particularly with blood platelets, it was demonstrated that extraction of lipids from cell membranes reveals a proteinaceous membrane skeleton composed principally of actin. Electron microscopic images of those membrane skeletons very closely resemble the cell

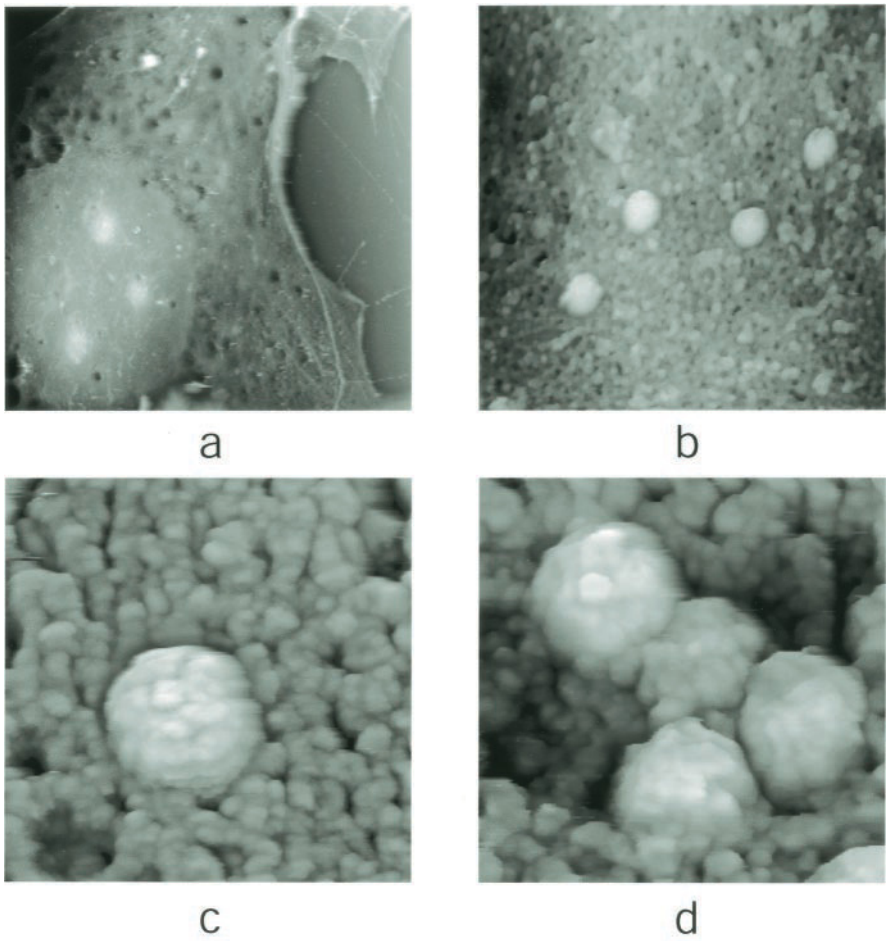

FIGURE 1 In (*a*) is a normal, uninfected National Institutes of Health 3T3 fibroblast imaged at low magnification by tapping mode AFM. The cells were fixed with glutaraldehyde and dehydrated with, and imaged under, ethanol. The bulging nucleus is clearly evident at this magnification. The lipid portions of the plasma membrane are lost by exposure to ethanol unless postfixed with OsO_4. Some membrane proteins and the membrane skeleton, however, likely remain on the cell surface due to glutaraldehyde fixation. In (*b*)–(*d*) is a series of tapping mode AFM images of virions emerging from the surfaces of MuLV-infected NIH 3T3 cells. The viral-infected fibroblasts have been fixed with glutaraldehyde and imaged under ethanol. The granular background is composed of cellular proteins on the surface of the cell. In many of these images, though of only moderate magnification, protein units can be seen forming a substructure on the surfaces of the virions. Scan areas: (*a*) $40 \times 40\ \mu^2$, (*b*) $2 \times 2\ \mu^2$, (*c*) $300 \times 300\ nm^2$, (*d*) $430 \times 430\ nm^2$.

surface structure that we observe by AFM, and are presumably the same.

Because each cell has displayed on its surface many emerging virions, it presents an array of particles at all stages of the budding process. These can be discriminated by their heights above the surface of the cell, those initially budding exhibiting low heights, and mature virions having the full height of a particle. A series of virions at different stages of budding are presented in Fig. 2, *a–d*. It is also noteworthy that the cell surfaces are pocked with pores which pass to the interior. Some pores are either much smaller or much larger than single virus particles and may be inherent structural elements of the cell surface. An unusually high proportion, however, are exactly within the range of diameters of MuLV virions, and some have a distinctive crown, or cusp appearance, as though created by the expulsion of some particle or material. Examples are seen in Fig. 2, *e* and *f*. We suspect that these crater-like pores may mark the sites of recently emergent virus particles.

In the images of Fig. 1, *b–d*, recognizable virions can indeed be seen associated with the cell surface, and these have appearances very similar to those of virions spread on mica. In general, virions associated with cell surfaces are more clearly imaged and are more distinctive because they are better immobilized and less sensitive to the scanning tip. Occasionally the budding virions appear in groups, and are virtually in contact with one another, but often individually as well. We did not, in broad scans over entire cell surfaces, observe any pronounced clustering of the budding virions. This suggests that no specific regions of the cell surface favor, or are reserved for, virus assembly, maturation, and budding.

Fig. 3, *a–d* contains images of MuLV virions at higher magnification. The virions do not have a regular external

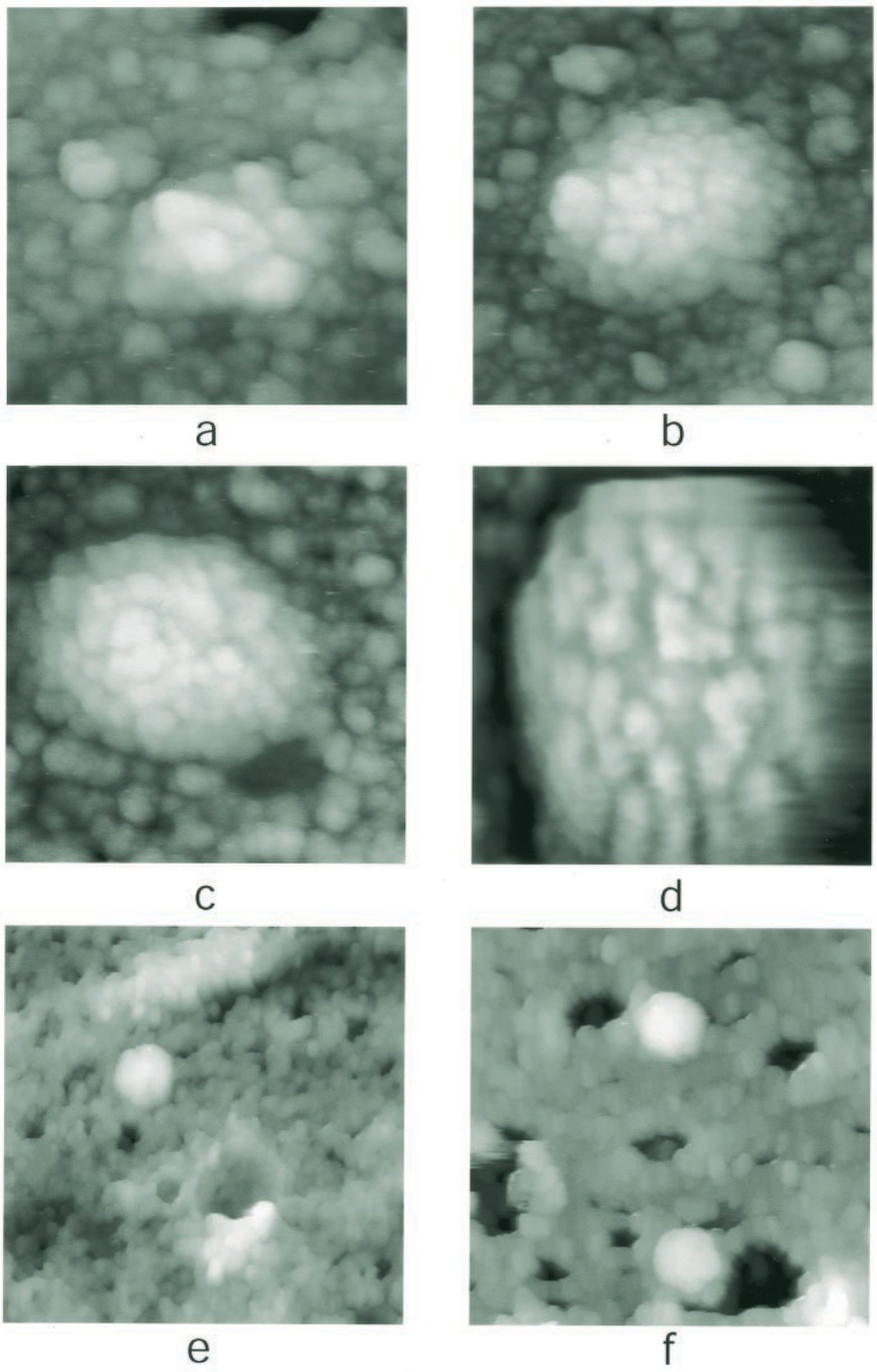

FIGURE 2 In (*a*)–(*d*) are images of MuLV virions at different stages of emergence from the surface of an infected cell. The heights of the particles above the cell surface are (*a*) 30 nm, (*b*), 40 nm, (*c*) 50 nm, and (*d*), 140 nm. In (*e*) and (*f*) are AFM images of small areas of MuLV-infected cells showing not only the emergence of newly assembled virions, but pores exhibiting cusps suggestive of recent virion departures. The sizes of the pores and craters correspond well with the sizes of the virions. Viruses in (*a*)–(*d*) have been postfixed with OsO_4. Scan areas are (*a*)–(*d*) 200 × 200 nm^2, (*e*) 1 × 1 μ^2, and (*f*) 820 × 820 nm^2.

structure that is consistent from particle to particle, as we find in more geometrically based virus capsids, as exemplified by icosahedral and helical arrangements. The surfaces of the virions in these images, it must be remembered, however, do not represent the protein capsid containing the RNA, which is buried deeper within the particle. The surfaces we observe here with AFM are, presumably, a consequence of the organization of the integument proteins that

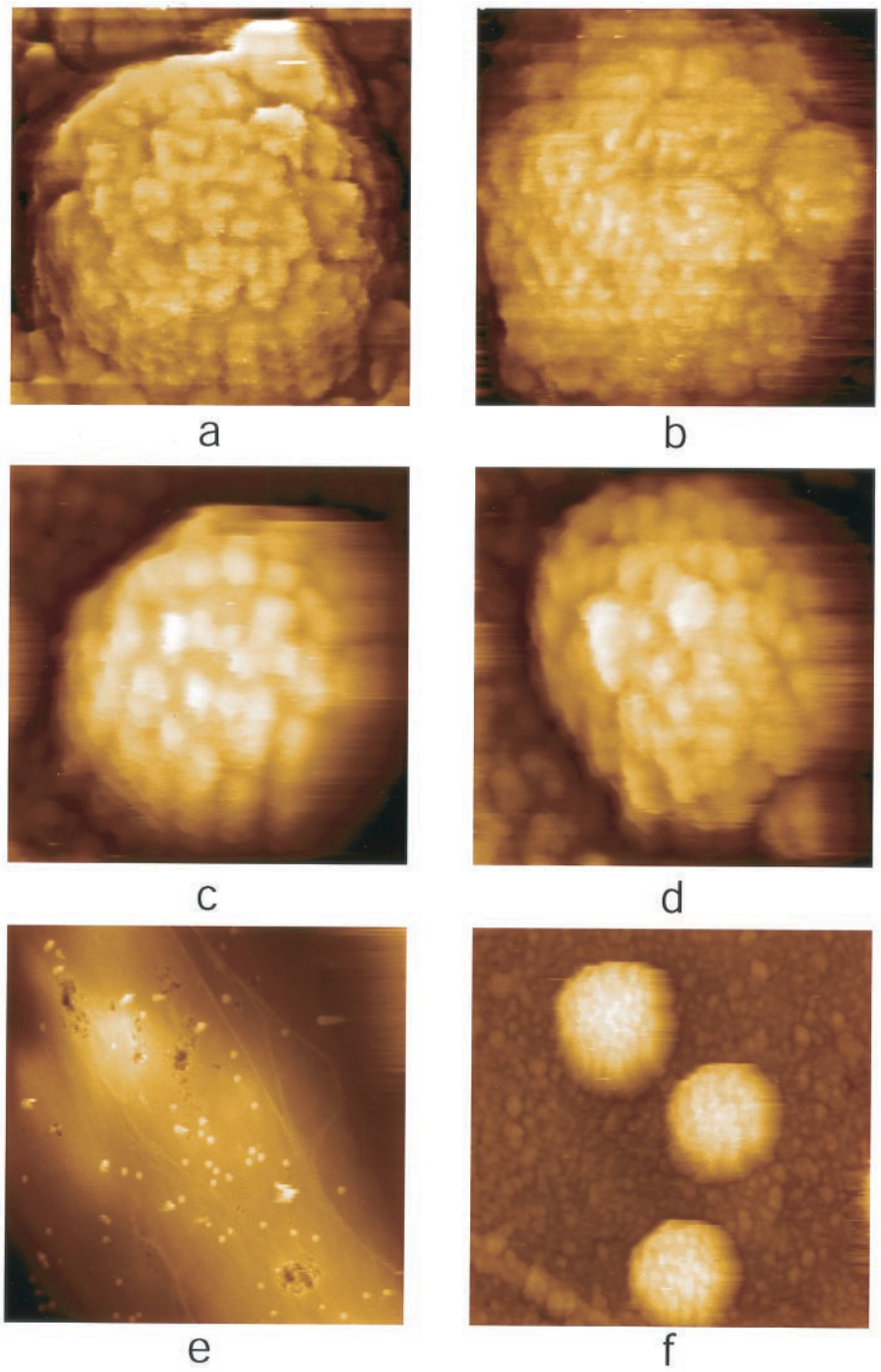

FIGURE 3 In (*a*) and (*b*) are high magnification AFM images of virions observed on the surfaces of infected cells when glutaraldehyde fixed and exposed to ethanol. These images are typical of many such images recorded from numerous samples of infected cells. The observed surface structure of the virions is difficult to characterize, as it shows little regularity. Individual protein units are, however, clearly seen to make up the surfaces. Because no postfixation with OsO_4 was carried out, the lipid portions of the membranes are removed. Scan areas: (*a*) 190 × 190 nm^2, (*b*) 164 × 164 nm^2. When cells and viral particles are fixed with glutaraldehyde and postfixed with OsO_4, the lipid components of the membranes remain intact. In (*c*) and (*d*) are virions emerging from the cells, presumably with intact envelopes. In (*e*) and (*f*) are lower magnification AFM images of the postfixed NIH 3T3 cells infected with wild-type MuLV. The scan areas are (*c*) 200 × 200 nm^2, and (*d*) 200 × 200 nm^2, (*e*) 10 × 10 μ^2, (*f*) 550 × 550 nm^2.

lie between the membrane envelope and the more interior capsid, superimposed with embedded proteins of the viral membrane.

Postfixation of cells and virus with OsO_4 maintains the lipid components of membranes and envelopes and produces somewhat different images of the samples. An OsO_4-fixed cell is seen at lower magnification, in Fig. 3, *e* and *f*, to be smooth, reflecting the presence of the lipid bilayer. At higher magnification, proteins embedded in the lipid matrix, however, produce a much coarser and irregular appearance. In particular, the networks of chains of protein subunits characteristic of membrane skeletons are no longer evident. The virions also appear somewhat different as well, but still closely resemble the non-OsO_4-treated virions.

Although irregular in detailed architecture, the MuLV virion surfaces do have certain similarities that are worth noting. The virions are of about the same overall size, 80–150 nm in diameter, all are roughly spherical in shape,

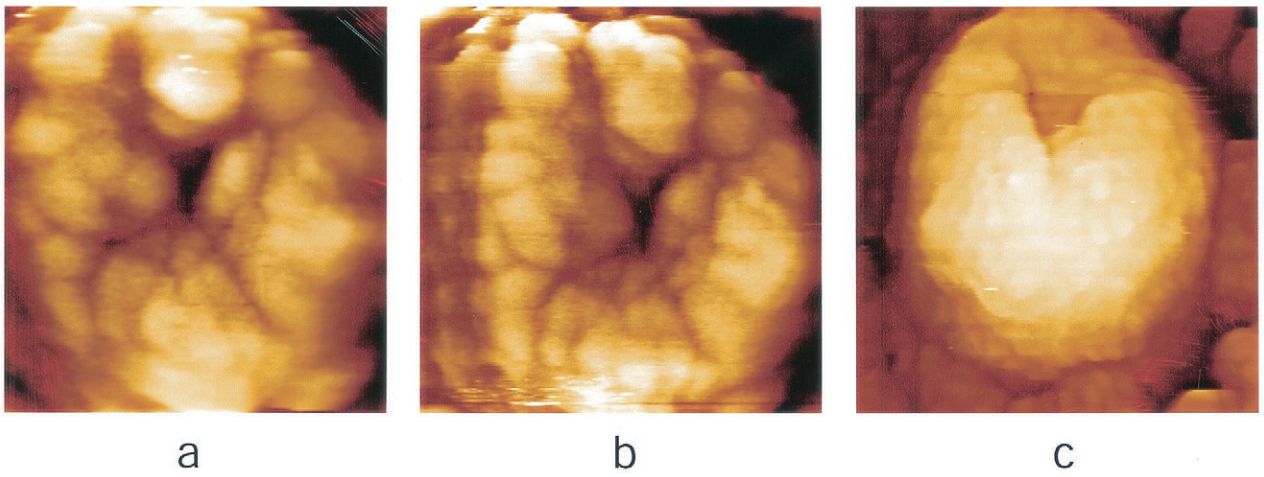

FIGURE 4 In (*a*) and (*b*) are two successive AFM scans of the same MuLV virion demonstrating the constancy of surface features and the reproducibility of the AFM technique. The virions in (*a*)–(*c*) are defective or damaged and a sector of surface proteins is missing in each case, resulting in a cavity and channel leading deeper into the interior of the virus particle. Scan areas: (*a*) 200 × 200 nm^2, (*b*) 200 × 200 nm^2, (*c*) 300 × 300 nm^2.

and all exhibit a variegated topological structure. Distinctive units, presumably individual proteins, or assemblies of proteins, are massed together to produce flowerlike appearances. A globular protein substructure is, however, clearly evident on all virions.

The irregularity of the virion surfaces is not due to softness, nor to mobility or fluidity, which would render scanning uncertain and yield ambiguous images. It is also not a consequence of any irreproducibility in the AFM technique itself. This can be demonstrated by repetitive scanning of the same particle, or by scanning the same particle in different directions. When this is done, the images are essentially the same. In Fig. 4 *a*, for example, is an incomplete, damaged, or defective virion in which some cluster of proteins is missing from the surface, thereby leaving a cavity. In this image some measure is obtained of the thickness and organization of the protein layer surrounding the capsid by inspection of the channel leading into the interior of the virion. Fig. 4 *b* is a second AFM scan of the same particle made minutes later. While not congruent, the two images are remarkably similar, particularly the shape of the cavity left by the missing proteins. Such defective virions, we noted, are not at all rare, and another is shown in Fig. 4 *c*.

Cells fixed with paraformaldehyde, which preserves the antigenicity of proteins, were immunolabeled with antibodies conjugated with 30 nm colloidal gold particles. Fig. 5 illustrates some results. The primary antibody was against the *env* surface protein of the virus. Because of their size, shape, and interaction with the tip, the gold particles are readily visible with AFM.

We also successfully carried out immunolabeling experiments using 15-nm-diameter gold particles, which provide greater resolution, and indeed in most circumstances these might be preferable. The protein clusters on the surfaces of the MuLV virions, however, are also ~15 nm in size, and

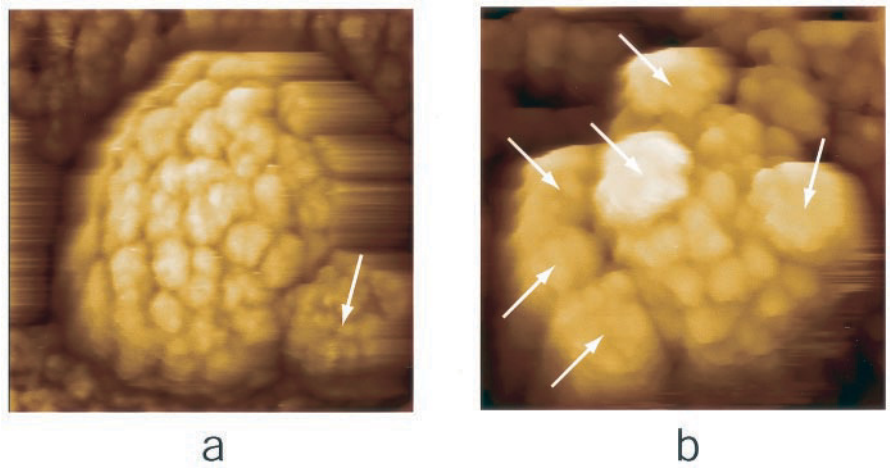

FIGURE 5 In (*a*) is an MuLV virion emerging from the surface of an NIH 3T3 cell, which is labeled with a single gold cluster-immunoglobulin conjugate. A coated particle of colloidal gold is seen at lower right and is marked with an arrow. In (*b*) is another MuLV virion labeled with six colloidal gold particles, again marked with arrows. The primary antibody was against the *env* protein of the virus surface.

initially this resulted in some ambiguity. To eliminate any question of what was a gold particle and what was not, the larger gold clusters were used.

In Fig. 5 *a* a MuLV virion on a cell surface has bound to it a single antibody-colloidal gold conjugate. In 5 *b* a single virion has six gold particles bound to its surface. Gold particles were also observed at some other locations on the cells' surfaces, though clearly the virus particles were strongly preferred. This may be due to the presence of *env* protein on the cell surface at early morphogenesis, where intact virion was not yet apparent, or due to free *env* protein on the cell surface. It may also have simply been due to nonspecific antibody or gold particle attachment. In any case, non-virion labeling was substantially reduced by first blocking the cells with goat serum before exposure to the primary antibody.

One implication of the labeling of the virions by the anti-*env* protein antibody is that the *env* protein is indeed present on the surfaces of the virions after fixation and dehydration. Though embedded in the virus membrane, they are not lost along with the lipid bilayer but remain, presumably along with matrix proteins, to cover the surface. We may further presume that the protein clusters of ~15 nm seen on the surfaces of the virions shown here, or at least some of them, are indeed composed of the *env* protein.

The AFM images to this point are typical of the many images of cells and virions obtained from 3T3 cells infected with wild-type MuLV. Fig. 6, again typical, contains corresponding images obtained from cells infected with MuLV mutant $gPr80^{gag}$, that mutation which produces an apparently defective, non-glycosylated, maturation protein. While some individual MuLV virions are occasionally still seen budding from the cell surface, they are few, and they are no longer the most prominent features. At low magnification the cell surfaces exhibit vast arrays of hairlike structures which, on closer inspection, are seen to be tubelike protrusions from the cells. The diameters of the tubes are quite uniform, and are about the same as those of wild-type virions. At one end, each tube is contiguous with the cell surface, while the distal ends are closed and rounded. They are not always linear, but frequently curve and twist. Their lengths vary greatly in a population, with the most common length being about a micron.

Fig. 7 presents linear composites of successive AFM images obtained from sequential scans over adjacent areas on single cell surfaces. The cells in these images were postfixed with osmium tetroxide. In these, the varied shapes and forms of the tubular protrusions are clear. Infection is high, yet there is a virtual absence of normal, budding virions. This, along with the observation that the tubes are absent on cells infected with wild-type virus, imply that the tubular structures must be derived from virions unable to experience normal morphogenesis. The tubes could conceivably arise from single virions unable to complete maturation and separation from the surface, thereby producing extended structures. Something similar has been seen, under different circumstances, for some simple defective plant viruses such as Alfalfa mosaic virus (Rossmann and Erickson, 1985; Mandahar, 1989) and some bacteriophages (Hendrix, 1985). Perhaps more significantly, the aberrant tubelike structures are reminiscent of late-domain mutants of MuLV (Yuan et al., 2000). However, the tubes may contain multiple virions, or capsids, like peas in a pod, or the linear arrangement of spores in neurospora filaments. We cannot be certain which of these is the case, or if both may pertain.

Further examination of these tubes in Figs. 6 and 7 shows the presence of a granular, protein substructure making up the surfaces. At high magnification, as in Fig. 6 *f*, the surfaces of the tubes begin to assume the crenulated appearance characteristic of the wild-type virion surfaces. Hence the tube surfaces may have the same protein composition as the surfaces of the wild-type, normally budding virions. In Fig. 6 *c* are a mass of tubes closely clustered on the cell surface, illustrating the high density that may occasionally occur. In Fig. 6 *d* is a more unusual event, a completed tube, which is closed at both ends and has somehow parted from the cell, but which still lies on its surface. Fig. 6 *f* is a high-magnification AFM scan of a single tube showing the irregular arrangement of protein units covering the surface.

DISCUSSION

We have not yet found a means to observe, with AFM, living cells in culture that are infected with virus, and which permit us to visualize accurately the cell surface without deformation or the interference of subsurface structure. Using the methods proven here, however, we can readily delineate the surface character of lightly fixed, dehydrated cells. Virions emerging from the cell surface are then visible, and their structures appear to be well preserved and undistorted. Features on the cell surface associated with virus budding, such as the cratered pores, also are clearly discerned.

Cells infected with wild-type virus display vast numbers of budding virions over their surfaces, with no particular distribution favored. No tubular structures are seen. Cells infected with virus carrying the $gPr80^{gag}$ mutation, however, express very few individual virions on their surfaces, but extensive arrays of tubular structures having diameters roughly that of MuLV virions. The tubular features have surfaces that appear similar in structure to the surfaces of wild-type virions. The tubular structures are undoubtedly associated with defective morphogenesis of the mutant virions arising from the non-glycosylated $gPr80^{gag}$ protein.

As already noted, we cannot be certain whether the tubular structures contain exclusively one, or several, capsids containing nucleic acid. Our feeling, however, is that they most likely contain a single infectious capsid. We base this on observations of many tubelike structures which seem to have a more dense, enlarged head at their

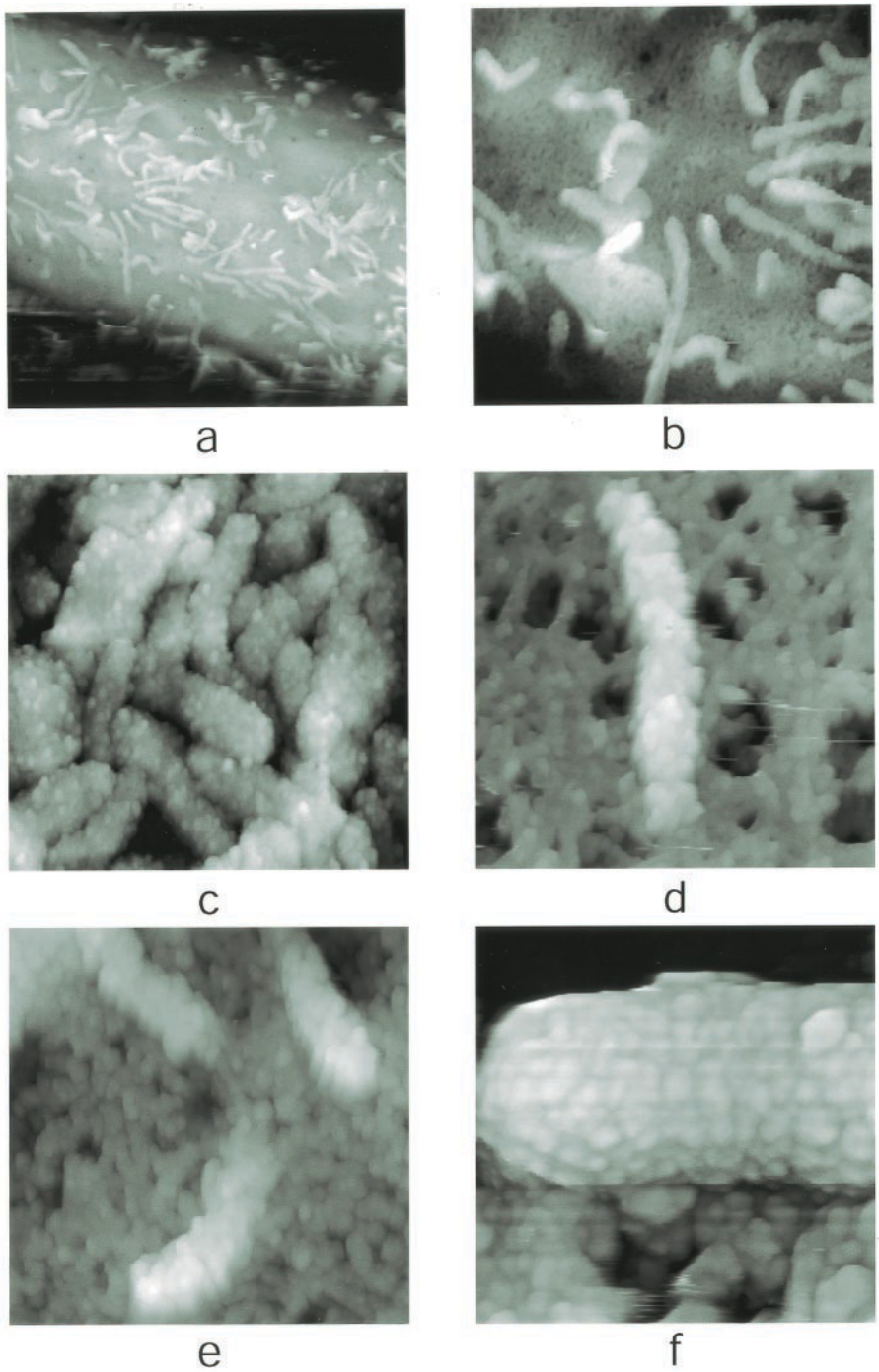

FIGURE 6 In (*a*) and (*b*) are AFM images of NIH 3T3 cells infected with the mutant virus $gPr80^{gag}$. The virions of the mutant are unable, in general, to properly mature and separate from the cell and instead form prominent tubelike protrusions from the cell surfaces. The cells and virus were fixed with glutaraldehyde and imaged under ethanol, so the lipid components of the plasma membrane are removed. Scan areas are (*a*) $30 \times 30\ \mu^2$, (*b*) $10 \times 10\ \mu^2$. In (*c*) is a mass of the tubelike structures that appear on the surfaces of cells infected with the $gPr80^{gag}$ mutant virus. This cell has been postfixed with OsO_4. In (*d*) through (*f*) are some individual tubules seen at higher magnifications, but after fixation only with glutaraldehyde before exposure to ethanol. In (*f*) the protein substructure of the tubule surface is beginning to appear. Scan areas: (*c*) $1 \times 1\ \mu^2$, (*d*) $1 \times 1\ \mu^2$, (*e*) $1 \times 1\ \mu^2$, (*f*) $300 \times 300\ nm^2$.

distal, closed ends, and usually, rather thin intervening regions along the tube. They have, in some cases, a cometlike appearance. These long tubes are not, so far as we can see, segmented, or periodically swollen in a way that would suggest any interior linear arrangement of capsids. Finally, there is no reason why multiple capsids would, or could, be assembled at identical points on cell surfaces and line up in a sequential fashion in the tube interiors. However, we occasionally see exceptions, which are consistent with the alternative.

It would have been satisfying to find some regular geometric arrangement of the protein units on the surfaces of wild-type virions and aberrant tubelike structures, but the images fail to support that. The virions appear to be polymorphic. This polymorphism could be due to an irregular or arbitrary distribution of the *env*

FIGURE 7 In (*a*) and (*b*) are composite images of the surfaces of two cells infected with the $gPr80^{gag}$ mutant virus and carrying the many tubelike protrusions on their surfaces. The image in (*a*) is compiled from five successive, adjacent scans with some small overlap area to permit joining. The horizontal discontinuities evident along the vertical edge of the image mark the boundaries of the successive scan images. The small horizontal shifts required to effect exact continuity were necessary to compensate for the natural drift of the instrument. Using this image composition method high-magnification images of rather large areas are possible. In (*b*) the image is composed from three successive, higher-magnification scan images. Both of the cells and their viruses were postfixed with OsO_4, after glutaraldehyde fixation, but before ethanol exposure. Hence, the cells and tubes both contain the lipid components of their membranes. Scan areas $2 \times 8.44\ \mu^2$, (*b*) $2 \times 4.72\ \mu^2$.

protein embedded in the lipid envelope, an arbitrary composition and arrangement of cellular membrane proteins acquired when the virion buds through the cell membrane, or it could be due primarily to an irregular arrangement of underlying integument proteins which the membrane overlays.

There is a visible difference in cell surfaces that have been fixed with glutaraldehyde alone and cells that have been postfixed with OsO_4 before dehydration. While appearing smoother at low resolution, cells exposed to OsO_4, which maintains lipid components of the membranes, exhibit a much rougher and topologically variable structure at high resolution. They are coated with distinctive bumps and small protrusions against an overall veiled surface. The rough appearance is presumably produced by the many membrane proteins embedded in the lipid matrix. The observation that this rough surface is, for the most part, lost in the absence of OsO_4 postfixation implies that many of the membrane proteins may be lost to the ethanol along with lipids during the dehydration process. The surfaces seen when only glutaraldehyde fixation alone is used are, therefore, primarily a consequence of the layer of protein components forming the membrane skeleton or lying immediately below the plasma membrane.

This work was supported by National Institutes of Health grants (to H.F. and A.M.), and a grant to A.M. from NASA.

REFERENCES

Bennett, V., 1982. The molecular basis for membrane-cytoskeleton association in human erythrocytes. *J. Cell. Biochem.* 18:49–65.

Cann, A. J., 1999. Virus Culture: A Practical Approach. Oxford University Press.

Coffin, J. M., 1992. Structure and Classification of Retroviruses. The Retroviridae. J. A. Levy, editor. Plenum Press, New York.

Edwards, S. A., and H. Fan. 1979. gag-Related polyproteins of Moloney murine leukemia virus: evidence for independent synthesis of glycosylated and unglycosylated forms. *J. Virol.* 30:551–563.

Evans, L. H., S. Dresler, and D. Kabat. 1977. Synthesis and glycosylation of polyprotein precursors to the internal core proteins of Friend murine leukemia virus. *J. Virol.* 24:865–874.

Fan, H., H. Chute, et al. 1983. Construction and characterization of Moloney murine leukemia virus mutants unable to synthesize glycosylated gag polyprotein. *Proc. Natl. Acad. Sci. U.S.A.* 80:5965–5969.

Fine, D., and G. Schochetman. 1978. Type D primate retroviruses: a review. *Cancer Res.* 38:3123–3139.

Fujisawa, R., F. J. McAtee, et al. 1997. Characterization of glycosylated Gag expressed by a neurovirulent murine leukemia virus: identification of differences in processing in vitro and in vivo. *J. Virol.* 71:5355–5360.

Gardner, M. B. 1980. Historical Background. Molecular Biology of RNA Tumor Viruses. J. R. Stephenson, editor. Academic Press, New York.

Gross, L. 1951. Spontaneous leukemia developing in C3H mice following inoculation in infancy with Ak-leukemic extracts, or Ak-embryos. *Proc. Soc. Exp. Biol. Med.* 76:27–32.

Gross, L., 1970. Oncogenic Viruses. Pergamon, Elmsford.

Hanecak, R., S. Mittal, et al. 1986. Generation of infectious Moloney murine leukemia viruses with deletions in the U3 portion of the long terminal repeat. *Mol. Cell Biol.* 6:4634–4640.

Hartwig, J. H., and M. DeSisto. 1991. The cytoskeleton of the resting human blood platelet: structure of the membrane skeleton and its attachment to actin filaments. *J. Cell Biol.*, 112:407–425.

Hendrix, R. W. 1985. Shape determination in virus assembly: the bacteriophage example. Virus Structure and Assembly. S. Casjens, editor. Jones and Bartlett, Boston. 170–203.

Kuznetsov, Y. G., A. J. Malkin, et al. 1997a. Molecular resolution imaging of macromolecular crystals by atomic force microscopy. *Biophys. J.* 72:2357–2364.

Kuznetsov, Y. G., A. J. Malkin, et al. 2001. Imaging of viruses by atomic force microscopy. *J. Gen. Virol.* 82(Pt 9):2025–2034.

Kuznetsov, Y. G., A. J. Malkin, et al. 1997b. Atomic force microscopy studies of living cells: visualization of motility, division, aggregation, transformation, and apoptosis. *J. Struct. Biol.* 120:180–191.

Levy, J. A., 1992. The Retroviridae. Plenum Press, New York.

Lowey, D. R. 1985. Transformation and Oncogenesis: Retroviruses. Virology. B. N. Fields, editor. Raven Press, New York. 235–264.

Luciw, P. A., and N. J. Leung. 1992. Mechanisms of Retrovirus Replication. The Retroviridae. J. A. Levy, editor. Plenum Press, New York.

Mandahar, C. L., 1989. Multicomponent Viruses. Plant Viruses. C. L. Mandahar, editor. CRC Press, Boca Raton. 99–105.

Miller, A. D., and C. Buttimore. 1986. Redesign of retrovirus packaging cell lines to avoid recombination leading to helper virus production. *Mol. Cell Biol.* 6:2895–2902.

Murphy, F. A. 1985. Virus Taxonomy. Virology. B. A. Fields, editor. Raven Press, New York. 22.

Neil, J. C., D. E. Onions, et al. 1980. Polypeptides of feline leukaemia virus: identification of p15(E) and p12(E). *J. Gen. Virol.* 50:455–460.

Pincus, T. 1980. The Endogenous Murine Type C Viruses. Molecular Biology of RNA Tumor Viruses. J. R. Stephenson, editor. Academic Press, New York.

Price, J., D. Turner, et al. 1987. Lineage analysis in the vertebrate nervous system by retrovirus-mediated gene transfer. *Proc. Natl. Acad. Sci. U.S.A.* 84:156–160.

Rossmann, M. G., and J. W. Erickson. 1985. Structure and Assembly of Icosahedral Shells. Virus Structure and Assembly. S. Casjens, editor. Jones and Bartlett, Boston. 63–65.

Schultz, A. M., E. H. Rabin, et al. 1979. Post-translational modification of Rauscher leukemia virus precursor polyproteins encoded by the gag gene. *J. Virol.* 30:255–266.

Stephenson, J. R., editor. 1980. Molecular Biology of RNA Tumor Viruses. Academic Press, New York.

Wagner, E. K., and M. J. Hewlett. 1999. Basic Virology. Blackwell Science, Oxford.

Weiss, R. A. 1982. Experimental biology and assay of retroviruses. Molecular Biology of Tumor Viruses: RNA Tumor Viruses. R. A. Weiss, N. Teich, H. E. Varmus, and J. M. Coffin, editors. Cold Spring Harbor Laboratory Press, Cold Spring Harbor, NY. 209–260.

Weiss, R. A., N. Teich, et al., editors. 1982. Molecular Biology of Tumor Viruses: RNA Tumor Viruses. Cold Spring Harbor Laboratory Press, Cold Spring Harbor, NY.

Yuan, B., S. Campbell, et al. 2000. Infectivity of Maloney murine leukemia virus defective in late assembly events is restored by late assembly domains of other retroviruses. *J. Virol.* 74:7250–7260.